Simulation of reactor startup without external neutron source based on RMC

Conglong JIA[a*], Wu WANG[a], Kan WANG[a]
aDepartment of Engineering Physics, Tsinghua University, Beijing. 100084
*Corresponding author: jiacl@mail.tsinghua.edu.cn

1. Introduction

During the loading and startup process of pressurized water reactors (PWRs), it is essential to ensure critical safety by preventing the reactor from reaching an uncontrollable prompt critical state. To achieve this, effective monitoring of the fission rate is necessary. In many reactors, external neutron sources are placed during loading and startup to enhance neutron flux within the reactor core. This allows the neutron flux in the core to reach the lower limit of the detection range of monitoring systems, facilitating effective monitoring of the reactor. However, this startup method involving external neutron sources necessitates the procurement and comprehensive management of these sources, thereby increasing the costs associated with nuclear power construction and operation.

Nuclear reactor startup without external neutron source refers to the reactor startup process that involves initiating the reactor using only the neutrons generated from the spontaneous fission of nuclear fuel (such as uranium-238), without relying on external neutron sources. The entire startup process encompasses both loading and initiation stages. By adopting this startup approach, the reactor can avoid the drawbacks associated with using external neutron sources. This method helps reduce the costs of nuclear power construction and management while enhancing economic competitiveness.

While startup without external source offers several advantages, during the actual loading and startup process, the weak neutron field generated solely by the spontaneous fission of nuclear fuel can lead to challenges. The lack of a strong external neutron source makes it difficult for neutron flux detectors outside the core to effectively detect neutron signals, resulting in a monitoring "blind zone." In the event of an accident under these circumstances, a sudden introduction of a significant positive reactivity could lead to an unexpected core criticality or even an uncontrollable prompt critical state within a short period. This poses a risk to the safety of reactor.

This paper focuses on investigating the characteristics of the blind zone during reactor startup without external neutron source. Stochastic neutron kinetics requires DKS method for computational analysis. Firstly, the DKS method is improved within the RMC code. Subsequently, computational capabilities are developed to simulate the stochastic neutron kinetics phase during the startup without external source. Finally, specific reactor cases are analyzed through computational simulations to study the startup without external source in detail.

2. Research Method

2.1 Monte Carlo Direct Kinetics Simulation Method

Reactor startup without external neutron source is a process conducted in a weak neutron field, which necessitates analysis from the perspective of stochastic neutron kinetics. Stochastic neutron kinetics is theoretically described by the stochastic neutron transport equation. In 1958, Pal[1] and Bell established the stochastic neutron transport equation using the probability balance method[2], as shown in equation (1).

$$
\begin{aligned}
&\Omega \bullet \nabla G(z; \boldsymbol{x}, \boldsymbol{v}, t) + \frac{1}{v}\frac{\partial G(z; \boldsymbol{x}, \boldsymbol{v}, t)}{\partial t} = \sigma(\boldsymbol{x}, \boldsymbol{v}, t) G(z; \boldsymbol{x}, \boldsymbol{v}, t) \\
&- \sigma(\boldsymbol{x}, \boldsymbol{v}, t) \times \left[c_0(\boldsymbol{x}, t; \boldsymbol{v}) + \int c_1(\boldsymbol{x}, t; \boldsymbol{v} \to \boldsymbol{v}_1') \, G(z; \boldsymbol{x}, \boldsymbol{v}_1', t) \, d\boldsymbol{v}_1' \right. \\
&\left. + \iint c_2(\boldsymbol{x}, t; \boldsymbol{v} \to \boldsymbol{v}_1', \boldsymbol{v}_2') \, G(z; \boldsymbol{x}, \boldsymbol{v}_1', t) \, G(z; \boldsymbol{x}, \boldsymbol{v}_2', t) \, d\boldsymbol{v}_1' d\boldsymbol{v}_2' + \cdots \right]
\end{aligned}
\tag{1}
$$

$$
G(z; \boldsymbol{x}, \boldsymbol{v}, t) = \sum_{n=0}^{\infty} z^n p_n\left(R, t_f; \boldsymbol{x}, \boldsymbol{v}, t\right)
$$

Compared to the Boltzmann transport equation that describes neutron transport in strong neutron fields, the stochastic neutron kinetics equation is complex and exhibits nonlinear characteristics, making it difficult to solve using simple numerical methods. Stochastic neutron kinetics primarily focuses on the random behavior of a small number of neutrons. The Monte Carlo method initiates transport from the microscopic neutron level, which offers a natural advantage in capturing the stochastic nature of individual neutron behavior. Consequently, the DKS method is well-suited to describing the stochastic neutron kinetics process in a weak neutron field.

The DKS method is based on the first principle and explicitly simulates the evolution process of prompt and delayed neutrons in a time-dependent manner. This approach is a theoretically exact transient simulation method. As depicted in Figure 1, in the computational process of direct simulation, a fission reaction generates a corresponding number of neutrons, while a radiative capture reaction eliminates neutrons. This approach simulates neutron transport processes in a manner that closely mirrors real physical events.
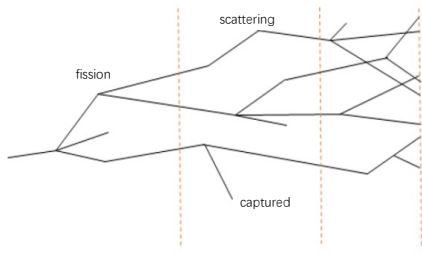
Fig. 1. Schematic representation of neutron transport using the DKS method

2.2 Function of reactivity over time

The startup of a real reactor is a dynamic process, with the reactivity changing over time. In deterministic methods, reactivity can be adjusted using data such as fission and absorption cross-sections. Monte Carlo is a high-fidelity simulation method, and the reactivity of real reactor changes mainly through two methods: the movement of control rods and the adjustment of boron concentration. In Monte Carlo simulations, the movement of control rods can be simulated by adjusting the position of specified surfaces, and changes in boron concentration can be simulated by altering the relative proportions of specified isotopes within the material.

In RMC, the linear interpolation method is employed to obtain the geometric parameters, material densities, and relative isotope proportions at specific time points. This implementation enables the functionality of geometric changes, material density adjustments, and changes in isotope compositions, as illustrated in Figure 2.
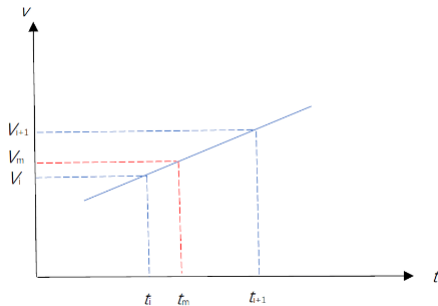

Fig. 2. Linear interpolation for system parameters

2.3 Transition time point calculation function

In the early stages of reactor startup, when there are a limited number of neutrons in the core, the application of stochastic neutron kinetics is necessary. As reactivity increases, the neutron population grows continuously until the point at which the system can be described using the average neutron population, allowing for the use of deterministic methods from classical reactor physics. Within the transition from stochastic to deterministic behavior, there exists a critical time point referred to as the transition time.

In deterministic analysis, the transition time is defined as the moment when the relative standard deviation (RSD) of the fission rate becomes stable. This is expressed as equation (2):

$$\text{RSD}(t) = \frac{F_\sigma(t)}{F_{ave}(t)} \tag{2}$$

In Monte Carlo simulations, the transition time is defined as the moment when the fission rate of the nuclear reactor system begins to exhibit exponential growth. Figure 3 illustrates the change in fission rate over time for a subcritical system undergoing delayed supercritical startup. During the initial period, the fission rate experiences significant fluctuations. As the neutron population increases, the fission rate starts to grow exponentially. For conservative estimation purposes, when the neutron fission rate surpasses a certain threshold value, it is considered that the neutron population begins to exhibit stable exponential growth. In the first plot of the figure, the designated fission rate threshold is 5×10^8 s^{-1}, corresponding to a transition time point of 27.3 seconds in the graph. Beyond this point, the neutron population enters a stable phase of exponential growth. Traditional transient analysis methods, such as Predictor-Corrector Quasi-Static methods (PCQS), can be employed to describe the system after this point. Thus, the determination of the transition time can be based on the time when the fission rate reaches the specified threshold.
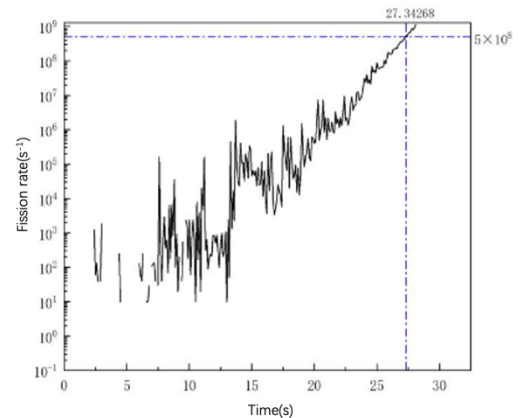

Fig. 3. Fission rate during delayed supercritical startup of a subcritical system

3. Test introduction

This paper focuses on the simulation and analysis of specific reactor startup without external neutron source. Due to the time-consuming nature of the DKS method, small-sized reactors are chosen for the calculations. Moreover, aligning with international research trends, the KRUSTY (Kilowatt Reactor Using Stirling TechnologY) heat pipe-cooled reactor is selected as the research subject for simulation analysis. KRUSTY is a novel reactor design that employs alkali metal high-temperature heat pipes to remove fission heat from the core. It offers advantages such as simple structure and high system reliability[3]. The radial cross-section of the reactor core is illustrated in Figure 4[4]. The reactor core, depicted in red, is a hollow annular cylinder (with inner

and outer diameters of 4 cm and 11 cm, respectively), standing at a height of 25 cm. The outer surface of the reactor core features eight columnar heat pipes. The reactor core is composed of a uranium-molybdenum alloy (8wt% Mo) weighing 32 kg, with a 93% enrichment level for ^{235}U.
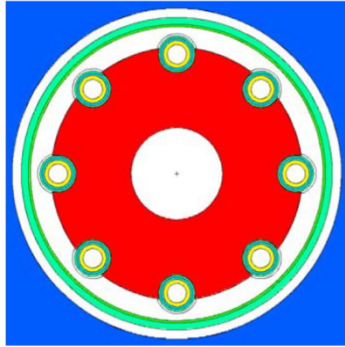

Fig. 4. Radial cross-section of the KRUSTY reactor core

The entire KRUSTY system is illustrated in Figure 5[5]. The core is positioned at the center, as depicted in the middle, and is surrounded by the purple shielding layer. Above, the Stirling engine is shown, while below is the core support platform and the beryllium oxide reflector layer's movable platform. As observed in Figure 5(a), the reflector layer is not inserted into the core, and in Figure 5(b), the reflector layer is inserted into the core from the bottom upwards. By adjusting the position of reflector layer, the reactivity can be regulated.
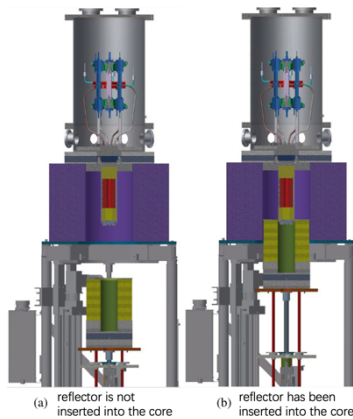

Fig. 5. Reflector layer movement in the KRUSTY system

Firstly, the RMC code is utilized for modeling. The radial cross-section of the core is illustrated in Figure 6, while the axial cross-section of the core is depicted in Figure 7. It is evident that in the current state, the reflector layer is fully inserted into the core, resulting in the maximum reactivity of the system.
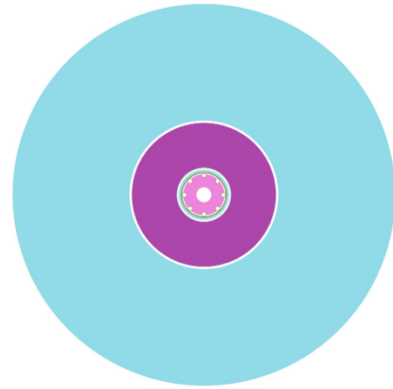

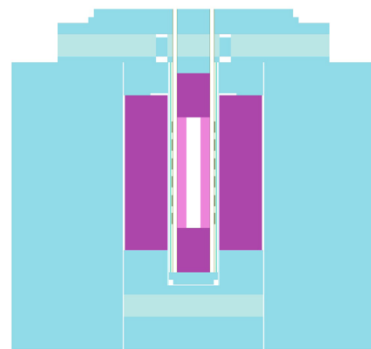Fig. 6. Radial cross-section modeling of KRUSTY using RMC

Fig. 7. Axial cross-section modeling of KRUSTY using RMC

4. Numerical analysis

4.1 Calculation of spontaneous fission source

In nuclear reactor startup without external neutron source, there are no externally introduced neutron sources; neutrons originate from the spontaneous fission of the nuclear fuel itself. Consequently, it's necessary to establish detailed source terms. As depicted in Figure 8, which showcases a radial segment of the reactor core constructed using RMC, the neutron source region (i.e., the nuclear fuel region) should be defined as the annular cylindrical area at the center of the image. Additionally, the eight columnar heat pipes on the outer periphery of the cylinder should be excluded.
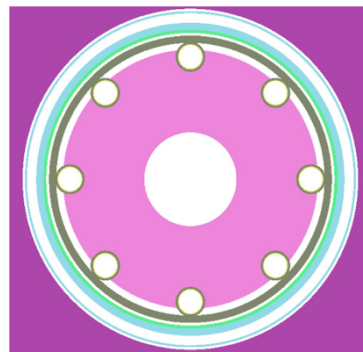

Fig. 8. Radial segment of the reactor core in RMC modeling

Considering the mass of isotopes within the fuel and their respective spontaneous fission yields, the total neutron source strength of the fuel can be computed as 36.37 n/s. The energy distribution of the spontaneous fission source is modeled using the Watt fission spectrum, while the angular distribution is assumed to be isotropic.

4.2 Numerical calculation results

The test case involves a step-reactivity of 0.33 $. The reactivity evolution over time is presented in Table 1: At 0 seconds, the reactivity is -6.04 $, at 1 second, the reactor reaches criticality, and at 2 seconds, the reactivity increases to 0.33 $, remaining constant thereafter.

Table 1. Reactivity evolution over time in the KRUSTY test case

Time/s	moving distance of reflector/cm	Reactivity/$
0	-10	-6.04
1	-5.3	0
2	-5	0.33

The variation of fission rate over time in a sample is shown in Figure 9. The probability distribution of the transition time is depicted in Figure 10. It's evident that the system has the highest probability (5%) of achieving the specified fission rate exactly at 188 seconds. Figure 11 illustrates the cumulative probability distribution of the transition time. Prior to 130 seconds, it's unlikely to reach the transition time; however, after 130 seconds, there's a possibility of reaching it. After 178 seconds, the likelihood of reaching the transition time surpasses 50%, and by 188 seconds, there is a 64% probability that the system will achieve the transition time.
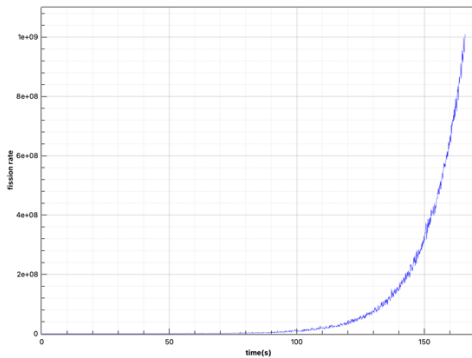

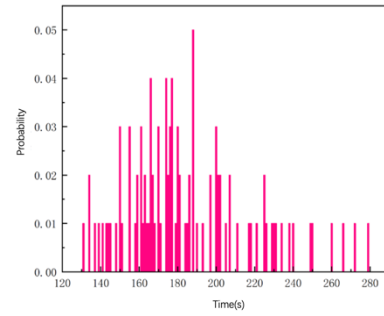Fig. 9. Fission rate change with time in the KRUSTY test case

Fig. 10. Probability distribution of transition time in the KRUSTY test case
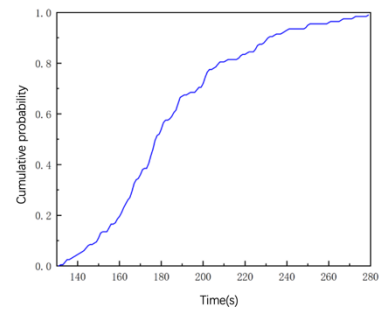

Fig. 11. Cumulative probability distribution of transition time in the KRUSTY test case

Subsequently, the position with the maximum neutron flux within the reactor core at various time points is analyzed, along with its probability distribution.

(1) Position of maximum neutron flux within the core at 50 seconds

The positions of the maximum neutron flux within the core at 50 seconds are presented in Table 2. Among all positions, the most frequent occurrence (highest probability) is associated with the fuel assembly sequence "1>6>129>140," with a probability of 71%. The visualization of the top three fuel assembly positions based on probability is depicted in Figure 12. It's noticeable that the regions with the highest neutron flux probability are close to the axial center and slightly towards the outer radial region.

Table 2. Probabilities of maximum neutron flux positions within the reactor core at 50 seconds

serial number	cell number	probability
1	1>6>129>140	71%
2	1>6>128>140	19%
3	1>6>130>140	3%
4	1>6>128>139	2%
5	1>6>127>140	2%
6	1>6>125>139	1%
7	1>6>129>139	1%
8	1>6>133>138	1%

Fig. 12. Maximum neutron flux positions within the reactor core at 50 seconds

(2) Position of maximum neutron flux within the core at 100 seconds

The positions of the maximum neutron flux within the core at 100 seconds are presented in Table 3. Among all positions, the most frequent occurrence (highest probability) is associated with the fuel assembly sequence "1>6>129>140," with a probability of 92%. The visualization of the top three fuel assembly positions based on probability is depicted in Figure 13. It's apparent that the regions with the highest neutron flux probability are slightly towards the outer radial region and close to the axial center, with a very small probability of occurring near the upper axial side.

Table 3. Probabilities of maximum neutron flux positions within the reactor core at 100 seconds

serial number	cell number	probability
1	1>6>129>140	92%
2	1>6>128>140	6%
3	1>6>132>139	1%
4	1>6>130>140	1%

Fig. 13. Layered depiction of the maximum neutron flux positions within the reactor core at 100 seconds

(3) Position of maximum neutron flux within the core at 150 seconds

The positions of the maximum neutron flux within the core at 150 seconds are presented in Table 4. Among all positions, the most frequent occurrence (highest probability) is associated with the fuel assembly sequence "1>6>129>140," with a probability of 90%. This probability is notably concentrated, potentially occurring in only two fuel assembly positions. The visualization of the two fuel assembly

positions with the highest probability is depicted in Figure 14. It's evident that the regions with the highest neutron flux probability are concentrated near the middle of the radial and axial directions, with a lesser probability of occurring at the upper axial side and the outer radial side. Therefore, particular attention should be paid to these two positions during the actual startup process or experiments.

Table 4. Probability distribution of maximum neutron flux positions within the reactor core at 150 seconds

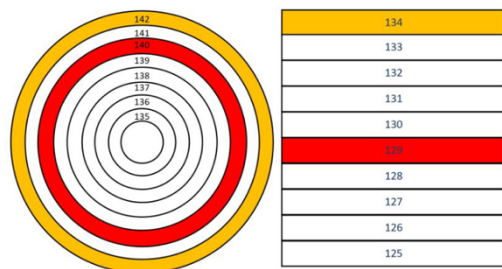| serial number	cell number	probability
1	1>6>129>140	90%
2	1>6>134>142	10%

Fig. 14. Maximum neutron flux positions within the reactor core at 150 seconds

5. Conclusions

This study utilized RMC to investigate the characteristics of reactor startup without external neutron sources. Through enhancements in Monte Carlo direct simulation kinetics capabilities, the evolution of reactivity over time was studied, and the calculation of transition points was explored. The analysis was conducted on the KRUSTY heat pipe reactor as a specific case. The reactivity of the system was computed for different geometries and materials, while the spontaneous fission source was described in detail. Furthermore, specific cases involving changes in reactivity were analyzed. The probability distribution of transition points and the spatial distribution of maximum neutron flux at specified times were computed for each scenario. These findings can provide valuable insights for addressing the blind phase in practical engineering applications, such as focusing on potential locations for the occurrence of maximum neutron flux. Overall, this work contributes to a better understanding of nuclear reactor startup without external neutron source and offers practical engineering guidance for such scenarios.

REFERENCES

[1] Pal L. On the theory of stochastic processes in nuclear reactors[J]. Nuovo Cimento (Italy)Divided into Nuovo Cimento A and Nuovo Cimento B, 1958, 10.
[2] Bell G I. On the stochastic theory of neutron transport[J]. Nuclear Science and Engineering,1965, 21(3): 390-401.

[3]柴晓明,马誉高,韩文斌,等.热管堆固态堆芯三维核热力耦合方法与分析[J].原子能科学技术, 2021, 55(S02): 7.

[4] Sanchez R G, Hutchinson J D, Mcclure P R, et al. Kilowatt reactor using stirling technology(krusty) demonstration. cedt phase 1 preliminary design documentation[R]. Los Alamos Na-tional Lab.(LANL), Los Alamos, NM (United States), 2015.

[5] Poston D I, Godfroy T, Mcclure P R, et al. Kilopower project-krusty experiment nuclear design[R]. Los Alamos National Lab.(LANL), Los Alamos, NM (United States), 2015.